Reduction of Flavins by Thiols. 2. Spectrophotometric Evidence for a Thiol-C(4a) Flavin Adduct and the Kinetics of Deprotonation of the -SH Group of the Dithiothreitol Adduct[1]

Edward L. Loechler*† and Thomas C. Hollocher*

Contribution from the Department of Biochemistry, Brandeis University, Waltham, Massachusetts 02254. *Received November 28, 1979*

Abstract: In the reduction of 3-methylriboflavin (**3**) by dithiothreitol (DTT) a second change in rate-determining step was observed at low [buffer] when [DTT] was low (5-mM range). The third sequential step thus revealed was buffer catalyzed, followed the rate law, k_{dc0}[B][HSSH][Fl], and is attributed to general-base (B)-catalyzed deprotonation of the -SH group of the C(4a) adduct between DTT and flavin. The Brønsted plot in the case of **3** for deprotonation of adduct -SH resembles that for simple proton transfer from thiols, except that the rate constants of the latter are larger by about 10^5. This factor of 10^5 is attributed to the unfavorable equilibrium of adduct formation, $K_{Add} \approx 10^{-5}$ M^{-1}. DTT monoanion was an effective general base in deprotonation of the adduct and exhibited the rate law k_{dc0}[HSS^-][HSSH][Fl]. A comparison of the deprotonation rate constants for **3** with those for 7-chlororiboflavin (**4**) and 7,8-dichlororiboflavin (**6**) gave $K_{Add} = 2.1 \times 10^{-4}$ and 3.4×10^{-3} M^{-1} for **4** and **6**, respectively. Difference spectra between **6** and **6** plus mercaptoethanol under conditions precluding net flavin reduction showed, in addition to solvent perturbations, the disappearance of a small fraction of **6** and the concomitant appearance of a new component with $\lambda_{max} \approx 370$ nm ($\epsilon \approx 15$ mM^{-1} cm^{-1}) by assuming the component to be formed stoichiometrically from **6**. $K_{Add} = 3.4 \times 10^{-3}$ M^{-1} agrees well with the value determined kinetically. Flavins **3** and **4** failed, as expected, to give spectrophotometric evidence for adduct formation. The difference spectrum showing the 370-nm component is similar to that of a form of lipoamide dehydrogenase ($\lambda_{max} = 387$ nm ($\epsilon = 8.7$ mM^{-1} cm^{-1})) which has been attributed to an adduct between flavin and an active site thiol. Implications of our findings to the mechanism of this and analogous enzymes are discussed.

Introduction

In the preceding paper,[2] the mechanism of the thiol-flavin reaction was established on the basis of kinetic results for the attack and breakdown steps. Deprotonation of the -SH group of the dithiol-flavin C(4a) adduct was inferred to be an essential step preceding breakdown.

In this paper, we show that the deprotonation step can be detected kinetically and shows buffer catalysis. In addition, spectral evidence is presented for formation of a C(4a) adduct between mercaptoethanol and 7,8-dichlororiboflavin (**6**).[3] The spectrum of the adduct resembles that observed by Thorpe and Williams[4] for the enzyme lipoamide dehydrogenase. Implications of the model reaction to the enzymic reaction are discussed.

Experimental Section

Spectra. Optical spectra of flavin-mercaptoethanol mixtures were obtained at room temperatures on a Varian Techtron 635 spectrophotometer equipped with a Sargent SRL recorder. At -16.2 °C spectra were obtained by using a Cary 14 spectrophotometer in which the cuvette block was chilled with circulating ethanol. The ionic strength of reaction mixtures containing several molar mercaptoethanol was not held at 1.0 for technical reasons.

Other materials and procedures were as described in the preceding paper.[2]

Kinetics—Reaction of Dithiol with Flavin. When three sequential steps are each partially rate determining and two of these are buffer catalyzed, then at constant pH eq 1 applies (Appendix I). This equation applies

$$1/k_2 = 1/(k_A + k_{AC}[\text{buffer}]) + 1/(k_D + k_{DC}[\text{buffer}]) + 1/k_B \quad (1)$$

for the reactants and conditions of this paper, including conditions at low pH at which thiol dianion attack was negligible (Scheme I, preceding paper).[2] The first, second, and third terms refer to the attack, deprotonation, and breakdown steps, resepctively. When all three terms were significant, a value for k_B was interpolated from the k_B pH rate profile (open circles, Figure 2, preceding paper).[2] Equation 1 can be rewritten as eq 2 and 3, where $1/k_{cor} = (1/k_2 - 1/k_B)$. Values for k_A, k_{AC}, k_D, and

$$k_{cor}' = [1/k_{cor} - 1/(k_A + k_{AC}[\text{buffer}])]^{-1} = k_D + k_{DC}[\text{buffer}] \quad (2)$$

$$k_{cor}'' = [1/k_{cor} - 1/(k_D + k_{DC}[\text{buffer}])]^{-1} = k_A + k_{AC}[\text{buffer}] \quad (3)$$

k_{DC} were obtained by iteration on eq 2 and 3. Iteration was terminated when no further change (<5%) accrued in the values of the rate constants.

Data were obtained at one pH value for each buffer used, and the k_{DC} term was assumed to obey the following rate equation, as it did with DTT serving both as reductant and buffer

$$k_{DC}[\text{buffer}][\text{thiol}] = k_{dc0}[\text{HSSH}][\text{B}][\text{Fl}]$$

where B refers to the conjugate base of the buffer. k_{dc0} was calculated from

$$k_{dc0} = k_{DC}(F_{HSSH}F_B)^{-1} \quad (4)$$

where

$$F_{HSSH} = (1 + K_1/a_H + K_1K_2/a_H^2)^{-1}$$

In the absence of buffers other than DTT k_{AC} in eq 1 was negligible and eq 5 was applied where DTT is the buffer. Values for k_D, k_{DC}, and

$$1/k_{cor} = 1/(k_D + k_{DC}[\text{buffer}]) + 1/k_A \quad (5)$$

k_A were calculated by an iterative procedure similar to that applied to eq 1 (preceding paper[2]). With changing pH k_A obeyed eq 6 (preceding paper[2]), but with the $k_{a2}K_2/a_H$ term being negligible at pH ≤8.64. The value for k_D with varying pH was fit by $k_{d0} = k_D/F_{HSS^-}$. In catalysis of deprotonation, k_{DC} had contributions at low pH primarily from a term involving DTT monoanion (serving as a base) and obeyed

$$k_{dc0} = k_{DC}(F_{HSS^-}F_{HSSH})^{-1} \quad (6)$$

Reaction of Thiols with 7. Reaction of **7** with mercaptoethanol (ME) resulted in the initial formation of the corresponding flavin cation radical

† Address correspondence to E.L.L. at the Biology Department, Massachussetts Institute of Technology, Cambridge, MA 02139.

(1) Supported by grants from the National Science Foundation (Grants GB-29337A1, PCM74-04834, PCM76-21678) and by a training grant from the National Institutes of Health (Grant GM-212). We thank John Lambooy, Peter Hemmerich and Franz Müller for the flavin derivatives used in this study. We also thank William Jencks for many useful discussions.

(2) Part I: Loechler, E. L.; Hollocher, T. C., accompanying paper in this issue.

(3) The structure of flavins **1** through **8** can be found or inferred in the preceding paper.[2]

(4) Thorpe, C.; Williams, C. H. *J. Biol. Chem.* **1976**, *251*, 7726.

0002-7863/80/1502-7322$01.00/0

Table I. Values of k_D, k_{DC}, and k_A in the Reaction of DTT with **3**, **4**, and **6** at 25 °C and Ionic Strength 1.0 M (KCl)

flavin	total DTT, mM	pH	k_D, M^{-1} min^{-1}	k_{d_1},[a,b] M^{-1} min^{-1}	k_{DC}, M^{-2} min^{-1}	k_{dc_0},[b,c] M^{-2} min^{-1}	k_A,[d] M^{-1} min^{-1}
3	5-50	7.78	0.47	11.20	209	5220	1.70
	2.5-50	8.31	0.92	7.16	422	3780	2.87
	5-75	8.64	1.6	6.74	1020	5750	3.46
4	2-18	7.75	7.8	199	3510	9.32×10^4	13.3
6	3-10	7.61	61.8	2160	5.77×10^4	2.07×10^6	94.3

[a] $k_{d_1} = k_D/(F_{HSS^-})$. [b] The average k_{d_1} and k_{dc_0} for **3** were 8.4 ± 2.5 M^{-1} min^{-1} and 4920 ± 1020 M^{-2} min^{-1}, respectively. [c] $k_{dc_0} = k_{DC}/(F_{HSS^-}F_{HSSH})$. k_{dc_0} is for DTT monoanion as general base. [d] With use of eq 6, k_{a_0} = 1.4 M^{-1} min^{-1} and k_{a_1} = 11.1 M^{-1} min^{-1} for **3** by assuming k_{a_2} = 9.4 M^{-1} (preceding paper[2]).

at lower pH and the neutral flavin radical at higher pH as evidenced by their characteristic spectra.[5] The formation of the cation radical at low flavin concentrations[6] obeyed

$$-d[7]/dt = k_{obsd}[7]^2$$

For most of the reaction, isobestic points were observed at 375, 455, and 515 nm to indicate the presence of only **7** and its corresponding cation radical. Subsequent reduction of the radical cation was slow. The reaction also appeared to be second order in ME and obeyed

$$k_{obsd}/[ME] = k_L[ME]$$

Reaction of **7** with dithiothreitol (DTT) resulted in the immediate formation of the cation radical, followed by a slower, kinetically complex reaction to form the corresponding reduced flavin. Neither phase was analyzed quantitatively.

Difference Spectra. Matching, divided, 1-cm path length cuvettes were used for difference spectra. A difference base line was run with compartments unmixed. Then the thiol and flavin compartments in the sample cuvette were mixed, and the difference spectrum was run. Finally the compartments in the reference cuvette were mixed, and a second base line was obtained. The two base lines agreed in all cases within 0.004 OD units and assured that pipetting errors and net flavin reduction were negligible. Absolute spectra were run before and after mixing.

Extinction Coefficient of the Flavin–Thiol Adduct. From the spectrum of oxidized **6**, the difference spectrum of **6** *minus* adduct and K_{Add} the extinction coefficient of the adduct, ϵ_{Add}^{370}, was calculated from eq 7,

$$\epsilon_{Add}^{370} = \epsilon_{ox}^{445}(\epsilon_{ox}^{370}/\epsilon_{ox}^{445} + \Delta/K_{Add}[RSH]100) \quad (7)$$

where Δ is the magnitude of the difference spectrum in percent. It was assumed that the adduct does not absorb a 445 nm. K_{Add} was taken to be 3.4 mM^{-1} and ϵ_{ox}^{445}, 12.5 mM^{-1} cm^{-1}. Additional experimental details were described in the preceding paper.[2]

Results

A Second Change in Rate-Determining Step. Figure 1A shows the dependence of k_{obsd} on [DTT] in the absence of any buffers except DTT. The plots curve upward and indicate that the reaction under these conditions was no longer simply first order in DTT. Data from the lower curve in Figure 1A are replotted as the lower curve of Figure 1B, which shows the dependence of k_{cor} on [DTT]. The curve conforms to eq 5. This hyperbolic behavior is characteristic of a change in rate-determining step and is analogous to that seen in Figure 1 (preceding paper[2]). The limiting rate for the lower curve in Figure 1B corresponded to the rate constant expected for the solvent attack step at this pH. Little or no curvature is seen when DTT is supplemented with 25 mM morpholine (upper curve, Figure 1B). This curve lies above the limiting rate constant for the lower curve by the amount of catalysis provided by 25 mM morpholine in attack at this pH. A reasonable assignment for the rate constants k_D and k_{DC} is that of solvent- and buffer-catalyzed deprotonation of the –SH group of the adduct (eq 8). Results qualitatively similar to those of

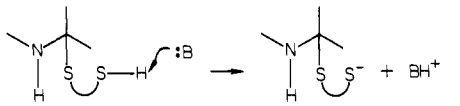

(8)

Figure 1B were observed at two additional pH values for the reaction of DTT with **3** and at one pH for both **4** and **6**. k_A was fit by eq 6 (preceding paper[2]). With DTT as the sole buffer, the buffer-catalyzed term, k_{DC} in eq 5, should represent deprotonation of the –SH of the C(4a) adduct by DTT monoanion. As expected this term obeyed

$$k_{DC}[DTT]^2[Fl] = k_{dc_0}[HSS^-][HSSH][Fl]$$

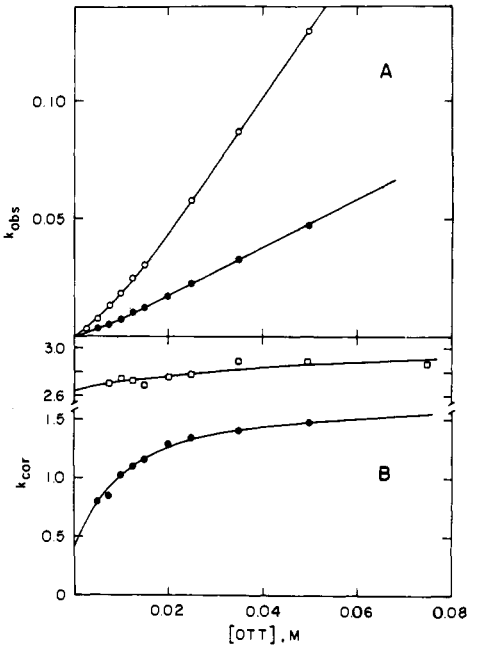

Figure 1. (A) Dependence of k_{obsd} on [DTT] in reduction of **3** at 25 °C and ionic strength 1.0 M (KCl): closed circles, pH 7.78; open circles, pH 8.31. The lines were fit to the data as described in the Experimental Section by using appropriate rate constants from Table I. (B) Dependence of $k_{cor} = (1/k_2 - 1/k_B)^{-1}$ on [DTT]: closed circles, replot of closed circles of A using k_B = 2.64 M^{-1} min^{-1} (the line was fit to the data as for A); open squares, data at pH 7.74 using k_B = 2.42 M^{-1} min^{-1} in the presence of 25 mM morpholine (a smooth curve was drawn through the data). Units are min^{-1} (A) and M^{-1} min^{-1} (B).

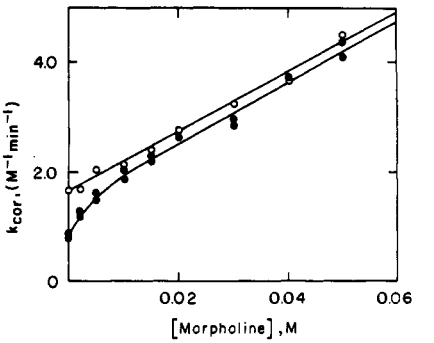

Figure 2. Dependence of $k_{cor} = (1/k_2 - 1/k_B)^{-1}$ on [morpholine] in reduction of **3** by DTT at 25 °C and ionic strength 1.0 M (KCl): solid circles, 5mM DTT, pH 7.74 (k_B = 2.42 M^{-1} min^{-1}) (the line was fit to the data as described in the Experimental Section by using k_A = 1.63 M^{-1} min^{-1}, k_{AC} = 56.4 M^{-2} min^{-1}, k_D = 1.61 M^{-1} min^{-1}, and k_{DC} = 1380 M^{-2} min^{-1}); open circles, 30 mM DTT, pH 7.74 (k_B = 2.42 M^{-1} min^{-1}) (the line was fit to the data by using k_A = 1.63 M^{-1} min^{-1} and k_{AC} = 54.4 M^{-2} min^{-1}).

(5) Kemal, C.; Bruice, T. C. *J. Am. Chem. Soc.* **1976**, *98*, 3955.
(6) At higher flavonium ion concentrations the reaction was no longer accurately second order.

Table II. General-Base-Catalyzed Rate Constants (k_{DC}) for the Deprotonation Step in the Reaction of DTT with 3 at 25 °C and Ionic Strength 1.0 M (KCl)

general base	pK	pH	k_{DC}, M^{-2} min^{-1}	k_{dco},[a] M^{-2} min^{-1}
potassium acetate	4.59	7.62	3.81	3.93
dipotassium phosphate	6.46	7.00	632	822
imidazole	7.25	7.68	985	1404
morpholine	8.92	7.74	1382	2.32×10^4
potassium dithiothreitolate	9.14	*b*	*b*	4920
potassium hydroxide	15.74			5.83×10^5 [c]

[a] Calculated from k_{DC} by assuming that the rate law for deprotonation is k_{dco}[HSSH][B][Fl]. [b] Values for k_{DC} at three pH values can be found in Table I. [c] Determined from the average value of k_{d1} (8.4 M^{-1} min^{-1}) from Table I.

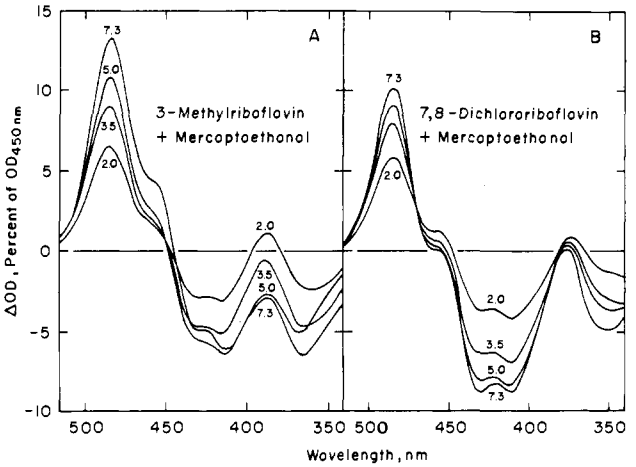

Figure 3. Difference spectra of **3** (A) and **6** (B) between water and ME/5 mM HCl at room temperature. The ordinate is the percent change in OD in the difference spectrum referenced to the initial OD of **3** at 448 nm (A) or **6** at 443 nm (B). Final [ME] were 2, 3.5, 5, and 7.3 M.

and was analyzed by using eq 6. k_D of eq 5 was determined at several pH values and obeyed

$$k_D[DTT][Fl] = k_{d0}[HSS^-][Fl]$$

to imply catalysis by hydroxide in the analogous solvent reaction. Data are summarized in Table I.

The change in rate-determining step from buffer-catalyzed deprotonation to attack, observed with DTT in Figure 1B, can be seen with other buffers such as with morpholine in Figure 2. At 30 mM DTT buffer catalysis was linear when corrected for breakdown, but at 5 mM DTT and at low [morpholine] a marked downward curvature was observed. These results are also explained by a change in rate-determining step from deprotonation at low [morpholine] to attack at higher [morpholine]. The lower curve in Figure 2 was fit by eq 9 derived from eq 1. Data are

$$1/k_{cor} = 1/(k_A + k_{AC}[buffer]) + 1/(k_D + k_{DC}[buffer]) \quad (9)$$

summarized in Table II. Because of the small range of buffer concentration that could be used to study the deprotonation step and the fact that this step was never more than 30–40% rate determining, the rate constants of Table II are considered to be accurate only within a factor of 2 to 4.

Difference Spectra of Flavins with ME. If a thiol–flavin adduct were formed in sufficient concentration, a difference spectrum should show the loss of some of the oxidized flavin and the formation of a new component.

Base line corrected difference spectra of **3** and **6** with ME in 5 mM HCl are shown in Figure 3. The low pH and aerobic conditions assured that reduced flavin did not form, as confirmed by the nearly identical base lines taken before and after mixing.[7]

(7) Formation of the adduct at this low pH would be rapid, because of the attack term k_{a0}[HSSH][Fl].

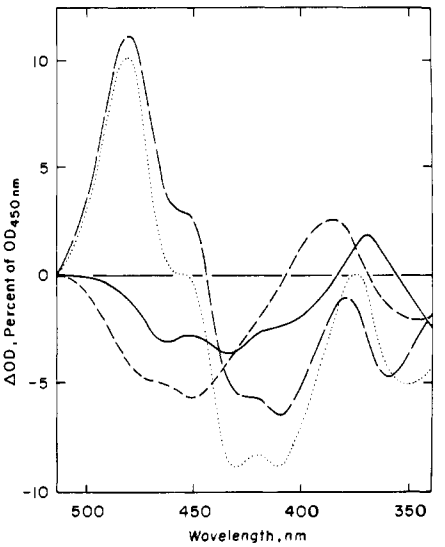

Figure 4. Difference spectra of flavins under various conditions: broken and dotted curves, difference spectra between water and 7.3 M ME/5mM HCl for **4** and **6**, respectively; solid curve, dotted *minus* broken curve; dashed curve, calculated difference spectrum between oxidized lipoamide dehydrogenase and mole fraction 0.06 of the corresponding (presumed) enzyme–flavin adduct.[4]

The prominent features are peaks at 485 and 375 nm and a double trough at 410 and 430 nm. This pattern is due largely to solvent perturbations of the oxidized flavin spectrum,[8] and qualitatively similar effects were seen with propanol and ethylene glycol.

The spectrum of an adduct must be resolved from solvent perturbations. Because electron-withdrawing groups on the electrophile are known in some cases to stabilize analogous adducts,[9,10] spectral resolution may be accomplished by comparing difference spectra of electron-withdrawing flavins (e.g., **6**) with those of otherwise identical flavins (e.g., **3** or **4**). Base line corrected difference spectra of **3** with ME are shown in Figure 3A. With increasing [ME] the peak at 485 nm increased, the double trough at 415 and 430 nm decreased, and the peak at 385 nm decreased. In contrast the peak at 375 nm for **6** (Figure 3B) decreased very little, as would be expected if a new species contributed in this region. In Figure 4 the base line corrected difference spectrum of **6** (dotted) is superimposed over that of **4** (broken). The difference in their difference spectra (solid) shows an increase in absorbance at 370 nm where an adduct is expected to absorb and a decrease in absorption around 450 nm as required in the conversion of oxidized flavin to adduct. **4** was used for comparison in Figure 4, because its oxidized spectrum (λ_{max} = 443, 356 nm) closely resembled that of **6** (λ_{max} = 443, 347 nm). The spectrum of **3** is less similar with peaks at 448 and 366 nm. However by displacing the difference spectrum of **3** to shorter wavelength by 5 nm and comparing it with that of **6**, we obtained a similar result. The dashed curve in Figure 4 shows the calculated difference spectrum between oxidized lipoamide dehydrogenase and the internal adduct (λ_{max} = 387 nm (ϵ = 8.7 mM^{-1} cm^{-1})) observed by Thorpe and Williams.[4]

In the case of **3** the position of the 450-nm band in the absolute absorption spectrum shifted to longer wavelengths upon addition of ME, but the absorbance at the maximum did not change. The absorbance decreased however in the case of **6**. In Figure 5 the percent decrease in OD of the 450-nm band is plotted against [ME]. For **6** a linear decrease was observed, while for **3** no change (or a slight increase) occurred. From these data a K_{Add} of 3.4 $\times$ 10^{-3} M^{-1} was calculated for **6** by assuming that the extinction coefficient of the adduct at 450 nm is zero. ϵ_{Add}^{370} was calculated

(8) Harbury, H. A.; Foley, K. A. *Proc. Natl. Acad. Sci. U.S.A.* **1958**, *44*, 662. Harbury, H. A.; LaNoue, K. F.; Loach, P. A.; Amick, R. M. *Ibid.* **1959**, *45*, 1708.

(9) Sayer, J. M.; Peskin, M.; Jencks, W. P. *J. Am. Chem. Soc.* **1973**, *95*, 4277.

(10) Ogata, Y.; Kawasaki, A. *J. Chem. Soc., Perkin Trans. 2* **1975**, 134.

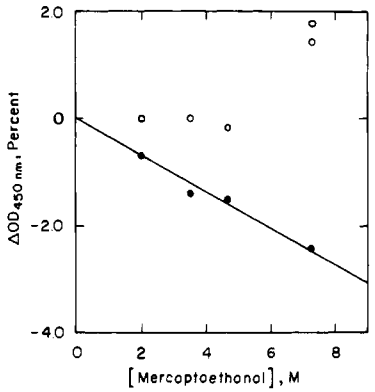

Figure 5. Percentage change in the absorption maximum of flavin near 450 nm as a function of [ME] at room temperature in 5 mM HCl: open circles, 3; closed circles, 6. The least-squares line through the closed circles has a slope of −0.0034 M^{-1}.

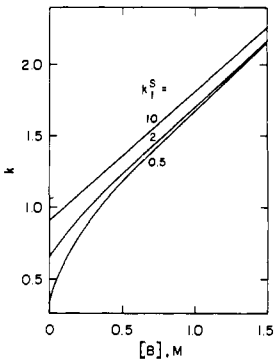

Figure 6. Computed curves for the situation wherein two sequential buffer-catalyzed steps are partially rate determining. The rate equation takes the form: $k = [1/(k_1^S + k_1^B[\text{buffer}]) + 1/(k_2^S + k_2^B[\text{buffer}])]^{-1}$. k_2^S, k_2^B, and k_1^B were assigned values of 1, 1, and 10, respectively. k_1^S was varied as indicated.

from eq 7 to be 15 mM^{-1} cm^{-1} with an error of about 50%.

Discussion

Adduct Deprotonation. When two sequential steps are buffer catalyzed and the buffer-catalyzed rate constant of one, k_1^B, is larger than the second, k_2^B, curvature in the buffer plots is observed only when the solvent rate constant $k_1^S < k_2^S$. This is illustrated in the theoretical curves of Figure 6. Curvature as in Figure 6 has been observed in the hydrolysis of the imine, 1,3-dimethyl-5-(*p*-tolylimino)barbituric acid by Sayer and co-workers.[11] At low buffer concentrations carbinolamine breakdown was rate determining, while at higher buffer concentrations water attack was rate determining and both steps showed buffer catalysis.

The lowest curve in Figure 6 is similar to the lower curve of Figure 2. Above 10 mM morpholine our data can be fit by a straight line which corresponds, as previously shown,[2] to an attack step. The curvature observed below 10 mM morpholine must therefore represent another partially rate-determining buffer-catalyzed step, which we take to be buffer-catalyzed deprotonation of −SH of the adduct. That curvature was lost with 30 mM DTT means that DTT can also catalyze this additional step. Catalysis of this step by DTT was confirmed by a term second order in DTT (Figure 1A,B, closed circles) which disappears at higher DTT concentrations where attack is rate limiting.

The data from Table II are plotted as general-base catalysis in the Brønsted plot of Figure 7 (lower curve) along with data from Eigen,[12] Kreevoy,[13] and Maass[14] (upper curve) for proton transfer from thiols.[15] The pK of the −SH of the DTT–flavin adduct should be nearly identical with the statistically corrected pK_1 for DTT of 9.44, and this value was used to determine the ΔpK values for our data. The straight lines of slope 1.0 and 0 meeting at $\Delta pK = 0$ (upper curve) were drawn for a diffusion-controlled step of 10^9 M^{-1} s^{-1} and thus define an "Eigen curve".[12] The solid line of slope 0.5 is the best straight line drawn through the open circles for proton transfer from thiol to thiolate. The Eigen curve and line of 0.5 slope were lowered by 5 log units to fit our data. Note that our points for phosphate and acetate fall approximately on the line of slope 1.0, that our point for hydroxide ion lies on the line of slope 0, and that our point for DTT lies approximately on the line of slope 0.5 as expected for proton transfer from thiol to thiolate.

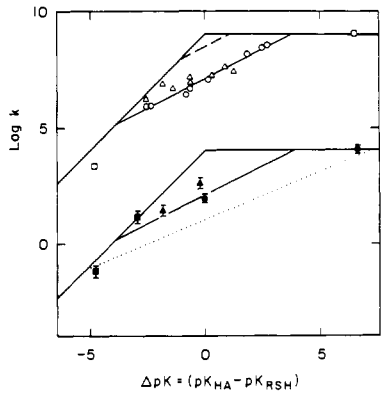

Figure 7. Brønsted plots for simple proton-transfer reactions from various thiols (open symbols) and for the deprotonation of the −SH group of the C(4a) adduct between 3 and DTT (closed symbols). Open symbols (M^{-1} s^{-1}) are taken from the literature;[12-14] closed symbols (M^{-2} s^{-1}) are from Table II. Circles, squares, and triangles are for proton transfer from thiol to sulfur, oxygen, and nitrogen bases, respectively. The upper Eigen curve (lines of slope 0 and +1) is drawn by assuming a diffusion controlled rate constant of 10^9 M^{-1} s^{-1}.[12] The line of slope 0.5 is the best straight line drawn through the data for proton transfer between sulfur atoms. The dashed line is for proton transfer between oxygen and nitrogen compounds (data not shown).[14] The lower Eigen curve was drawn 5 log units below the upper one to fit our data. The dotted line shows the relative position of the Brønsted plot for the attack step expressed as general-base catalysis (i.e., as k_{GB}[HSSH][A^-][Fl] rather than k_{acl}-[HSS^-][HA][Fl]).

Table III. Comparison of Rate Constants for the Deprotonization Step in the Reaction of DTT and 3 with Literature Values for the General-Base-Catalyzed Deprotonation of Mercaptoethanol

general base	k_{dco},[a] M^{-2} min^{-1}	k,[b] M^{-1} min^{-1}	(k_{dc}/k),[c] 10^5 M^{-1}
potassium hydroxide	5.83×10^5	$\sim 6 \times 10^{10}$	0.97
imidazole	1404	9.6×10^7	1.4
potassium acetate	3.93	1.2×10^5	3.3

[a] Data from Table II. [b] Values from ref 12 and 13. [c] Average is 1.9×10^{-5} M^{-1}.

In Table III data for the deprotonation step with hydroxide, imidazole, and acetate as general bases are compared with deprotonation of mercaptoethanol by the same bases. The ratios are given in the third column and agree within a factor of about 3. Considering the several literature sources of data and the uncertainties in our rate constants, this agreement is taken to indicate that the deprotonation step and thiol deprotonation are similar reactions.

Estimation of K_{Add}. For our deprotonation rate constants to be $\sim 10^5$ M lower than those of Eigen,[12] Kreevoy,[13] and Maass[14]

(11) Sayer, J. M.; Depecol, M. *J. Am. Chem. Soc.* **1977**, *99*, 2665.
(12) Eigen, M. *Angew. Chem., Int. Ed. Engl.* **1964**, *3*, 1.
(13) Kreevoy, M. M.; Sappenfield, D. S.; Schwabacher, W. *J. Phys. Chem.* **1965**, *69*, 2287.
(14) Maass, G. *Angew. Chem., Int. Ed. Engl.* **1968**, *7*, 818.

(15) Although the data of Eigen[12] and Maass[14] were collected at ionic strength 1.0 M, the temperature was 20 °C except for the deprotonation of ME by hydroxide which was at 25 °C. The pK for ME was taken by Maass to be 10.3 rather than 9.6. His pK for methyl mercaptoacetate at 20 °C (7.8) was similar to that reported at 25 °C by Jencks and Salvesen (7.91, ref 16). The rate constant for hydroxide ion deprotonation of ME (10^9 M^{-1} s^{-1}) was given by Eigen as approximate. The rate constant for ME deprotonation by acetate[13] applied at ionic strength 0.22 M (NaCl) and at 25–30 °C.
(16) Jencks, W. P.; Salvesen, K. *J. Am. Chem. Soc.* **1971**, *93*, 4433.

Scheme I

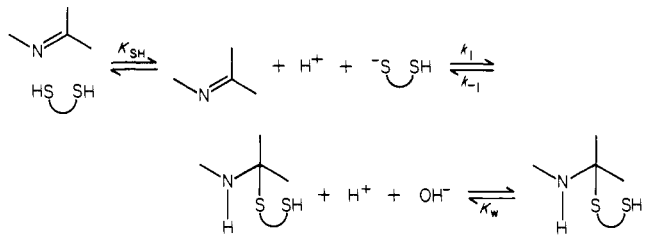

Table IV. Estimation of the Equilibrium Constant of Adduct Formation (K_{Add}) for 4 and 6 with DTT at 25 °C and Ionic Strength 1.0 M (KCl)

flavin	$(k_{d_1}^{Fl}/k_{d_1}^{3})^a$	$(k_{dco}^{Fl}/k_{dco}^{3})^a$	K_{Add},[b] M^{-1}
3	1.0	1.0	10^{-5}
4	23.8	19.0	$(2.1 \pm 0.3) \times 10^{-4}$
6	257	421	$(3.4 \pm 1.2) \times 10^{-3}$

[a] Rate constants are from Table I. The superscript Fl refers to the flavin in the indicated line, while the superscript 3 refers to 3-methylriboflavin. [b] K_{Add} is taken as the average of the two ratios in the preceding columns times 10^{-5} M^{-1}, the estimated K_{Add} for 3 (see text).

requires that proton transfer from sulfur be preceded by an unfavorable equilibrium, namely, that of adduct formation (see eq 10). The equilibrium constant (K_{Add}) must therefore be about 10^{-5} M^{-1}.

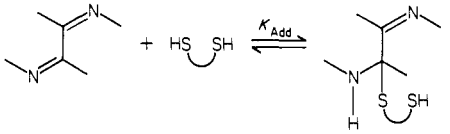

(10)

The dotted line in Figure 7 is the Brønsted plot for the *DTT attack step* (k_{acl}) shown as *general-base catalysis*. The rate constants for the deprotonation reaction are about one order of magnitude larger than for attack. This argues that K_{Add} can be no less than about 10^{-5}–10^{-6} M^{-1}, otherwise attack would not have been observed. Another lower limit for K_{Add} can be made from Scheme I, where the overall equilibrium is K_{Add} and $K_{Add} = (k_1 K_{SH}/k_{-1}K_w)$. Because $k_1 = 8.8$ M^{-1} min^{-1} (preceding paper[2]) and $k_{-1} \leq 10^{10}$ M^{-1} s^{-1} (the diffusion-controlled rate), $K_{Add} \geq 10^{-6}$ M.

Table I can be used to estimate K_{Add} for DTT with **4** and **6**. The ratios of k_D (or k_{DC}) for **4** or **6** to k_D (or k_{DC}) for **3** will reflect the ratios of K_{Add}, because all three adducts will have virtually identical –SH pK values. These ratios are tabulated in Table IV. A Hammett plot of log K_{Add} vs. flavin σ (see following paper[17] for assignment of σ values) gave a straight line with $\rho = 3.02$. This amounts to an increase of approximately one negative charge at N(5) in adduct formation considering that ρ is 2.8–2.89, 4.07, and 3.36 for anilinium,[18-20] aniline[21] and *N*-methylanilinium[22] ionizations respectively. This increase in negative charge at N(5) during the formation of the adduct amounts to another experimental verification of the fact that N(5) is electron deficient in oxidized flavin.

The equilibrium constants of adduct formation between DTT and flavin are much lower than, e.g., those between 2-methoxyethanethiol and acetaldehyde ($K_{Add} = 32$ M^{-1})[23] or between mercaptoethanol and the imine, *N*-(*p*-chlorobenzylidine)aniline ($K_{Add} = 18$ M^{-1}).[24] This may occur in part because adduct formation at C(4a) disrupts conjugation between the benzene and

Scheme II

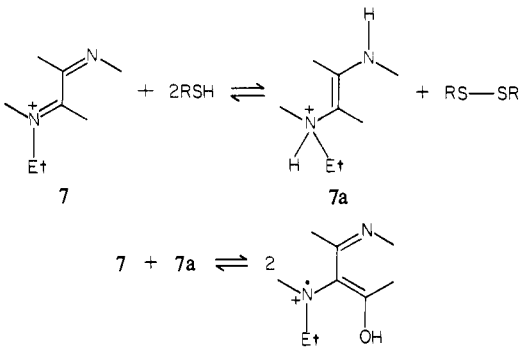

pyrimidine rings of flavin, with resulting loss of resonance energy. A similar conclusion was reached when considering the rate enhancement of $\sim 10^5$ in the hydrolysis of a nonplanar flavin model compound[11] and of $\sim 10^{10}$ in the essentially irreversible addition of thiolate to another such compound.[25]

The Absence of General-Acid Catalysis by DTT in Attack. The small increase in rate with increasing DTT concentration seen in Figure 1B in the presence of morpholine (open squares) is probably due to residual catalysis of deprotonation. But if this increase is used to set an upper limit to DTT acting as a general acid in attack (rate term k_{acl}[HSSH][HSS$^-$][Fl]), then $k_{acl} \leq 168$ M^{-2} min^{-1}. From the Brønsted plot of the preceding paper[2] a nitrogen or oxygen acid of similar pK would be expected to have $k_{acl} = 980$ M^{-2} min^{-1}. Thiol is at least a sixfold worse general acid in the attack step. From the data of Maass[14] simple proton transfer from thiol to nitrogen is about 15-fold slower than that between oxygen (or nitrogen) acids and bases (open triangles vs. dashed line in Figure 7). Thus in both general-acid catalyzed and simple proton-transfer reactions sulfur acids are less effective than oxygen or nitrogen acids. Also from the data of Maass[14] proton transfer between thiol and thiolate is slowed down only by an additional factor of <2 and not 15 (open triangles vs. open circles in Figure 7). It is not surprising, therefore, that thiolate can be an effective catalyst relative to oxygen or nitrogen base in the deprotonation of the –SH group of the adduct, as we observed.

Spectral Evidence for an Adduct. The equilibrium constants of adduct formation (Table IV) between DTT and **3**, **4**, and **6** are 10^{-5}, 2.1×10^{-4}, and 3.4×10^{-3} M^{-1}, respectively. If these constants were the same for ME (including statistical corrections but ignoring salt and solvent effects), then the percentage of adduct formed in 50% water/50% ME (7.3 M) would be 0.004%, 0.08%, and 1.2%, respectively. In difference spectra only **6** might show detectable levels of adduct, as was observed.

The kinetic value of K_{Add} for DTT (3.4×10^{-3} M^{-1}, Table IV) agrees well with the spectrophotometric estimate with ME (3.4×10^{-3} M^{-1}, Figure 5). For a comparison of these numbers the value for DTT must be halved because of its two –SH groups. In spite of differences in [salt] and solvents, these values for K_{Add} agree within a factor of 2.

All reported C(4a) adducts show $\lambda_{max} \geq 350$ nm,[26,27,30-32] whereas N(5) adducts show $\lambda_{max} \leq 355$ nm.[26-29] The difference maximum observed at 370 nm is thus more consistent with a C(4a) than with an N(5) adduct, but this assignment must be considered tentative because it has not been possible to obtain acceptable

(17) Part III: Loechler, E. L.; Hollocher, T. C., accompanying paper in this issue.
(18) Exner, O. "Advances in Free Energy Relationships", Chapman, N. B., Shorter, J., Eds., Plenum Press: New York, 1972; p 1.
(19) Biggs, A. I.; Robinson, R. A. *J. Chem. Soc.* **1961**, 388.
(20) Abrams, W. R.; Kallen, R. G. *J. Am. Chem. Soc.* **1976**, *98*, 7777.
(21) Dolman, D.; Stewart, R. *Can. J. Chem.* **1967**, *45*, 911.
(22) Stewart, R.; Dolman, D. *Can. J. Chem.* **1967**, *45*, 925.
(23) Lienhard, G. E.; Jencks, W. P. *J. Am. Chem. Soc.* **1966**, *88*, 3982.
(24) Sayer, J. M., personal communication.
(25) Sayer, J. M.; Conlon, P.; Hupp, J.; Fancher, J.; Belanger, R.; White, E. J. *J. Am. Chem. Soc.* **1979**, *101*, 1890.
(26) Hemmerich, P. "Flavins and Flavoproteins"; Kamin, H., Ed.; University Park Press: Baltimore, MD, 1971; p 83.
(27) Hevesi, L.; Bruice, T. C. *Biochemistry* **1973**, *12*, 290. Bruice, T. C.; Hevesi, L.; Shinkai, S. *Ibid.* **1973**, *12*, 2083.
(28) Müller, F.; Massey, V. *J. Biol. Chem.* **1969**, *244*, 4007.
(29) Müller, F. *Z. Naturforsch., B: Anorg. Chem., Org. Chem., Biochem., Biophys. Biol.* **1972**, *27B*, 1023.
(30) Kemal, C.; Bruice, T. C. *Proc. Natl. Acad. Sci. U.S.A.* **1976**, *73*, 995.
(31) Ghisla, S.; Entsch, B.; Massey, V.; Huslin, M. *Eur. J. Biochem.* **1977**, *76*, 139.
(32) Walker, W. H.; Hemmerich, P.; Massey, V. *Eur. J. Biochem.* **1970**, *13*, 258. Hemmerich, P.; Haas, W. "Reactivity of Flavins"; Yagi, K., Ed.; University Park Press: Baltimore, MD; 1975; p 1.

Scheme III

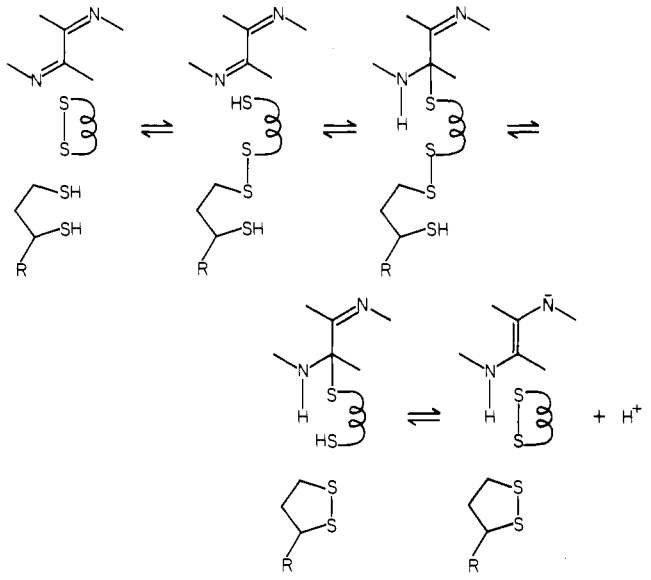

detailed spectra of the adduct. Similarities exist between the thiol–flavin adduct of lipoamide dehydrogenase (dashed curve) and the solid curve of Figure 4. Both show difference minima below the base line around 450 nm and maxima above in the 370–390-nm region.

While it is conceivable that the difference spectrum of the presumed adduct is due merely to a differential solvent effect between **4** and **6**, this interpretation is unlikely. The difference spectrum resembles that expected for known adducts and has a reasonable extinction coefficient. In addition its intensity increases in direct proportion to [ME] (unlike ordinary solvent effects),[8] and the corresponding decrease around 450 nm provides a K_{Add} value which agrees with that determined kinetically.

Because it was expected that a more electron-withdrawing flavin would show an even larger K_{Add}, evidence was sought for adduct formation between ME and **7**.

Reaction of Thiols with 7. Formation of the radical cation (see Experimental Section) probably involves dismutation (Scheme II). This scheme accounts for the fact that the reaction was second order in both **7** and ME. DTT yields reduced **7** faster than ME, because the equilibrium in the first step must lie further to the right. Slow conversion of the cation radical to reduced **7** probably begins by reversal of the second step. We failed to detect adduct formation with **7** even with 1 M ME in 7.3 M HCl at −16.2 °C. Reaction in dry acetonitrile similarly failed to yield adduct. An adduct was not observed because conditions favoring its formation (higher pH or [ME]) promote a faster overall reaction to yield the cation radical.

Implications for Enzyme Reactions. The thiol–flavin reaction is a model for several flavin mediated enzymes that transfer reducing equivalents between pyridine nucleotides and thiols.[4,33] This class of enzymes also contains an enzyme disulfide that has been shown to participate directly in the redox reaction.[34] Scheme III shows a reasonable mechanism for lipoamide dehydrogenase.

The first step is a thiol–disulfide interchange between enzyme-bound lipoamide and the enzyme disulfide. The second step involves the formation of the C(4a) flavin–thiol adduct. Thorpe and Williams[4] found that lipoamide dehydrogenase, with one of its thiols selectively alkylated with iodoacetamide, gave an adduct spectrum in the presence of NAD^+ which is similar to the adduct spectrum we observed, and both are consistent with C(4a) adducts.

The X-ray structure of glutathione reductase[35] shows that the proximal sulfur (Cys-46) of the enzyme disulfide touches the isoalloxazine ring at or close to C(4a). The distal sulfur (Cys-41) is in van der Waals contact with the disulfide of gluathione. A lysine nitrogen (Lys-49) on the side of flavin opposite that of Cys-41 and -46 touches near the oxygen of the C(4) carbonyl. Lys-49 could be the general acid responsible for proton transfer to the flavin N(5) position in attack. There is no way that electrons can be transferred directly between any of the thiols and pyridine nucleotide in glutathione reductase, because the flavin coenzyme lies between them. This is consistent with solution chemistry. NADH does not react with disulfides, but flavin can catalyze the reaction.[36] Disulfides can be reduced by hydride-transfer reagents such as sodium borohydride.[37] It has been suggested that enzymatic NADH reactions may proceed in two steps, possibly electron transfer followed by hydrogen atom transfer, rather than by hydride transfer.[38] If this were the case, poor reactivity with disulfides might be explained by the instability of some radical intermediate such as the disulfide radical anion.[39] This might explain why the thiol–pyridine nucleotide redox enzymes have evolved to contain a mediating flavin, which is capable of carrying out a radical-like reaction with one species (pyridine nucleotide) and a group-transfer reaction with the other (thiol).

Appendix I.

Derivation of the Overall Rate Constant for Steady-State Sequential Reactions of Any Length. For the sequential reaction of three steps

$$A + B \underset{k_{-X}}{\overset{k_X}{\rightleftharpoons}} X \underset{k_{-Y}}{\overset{k_Y}{\rightleftharpoons}} Y \xrightarrow{k_Z} Z$$

the observed second-order rate constant k_2 equals $(k_X P_{XZ})$, where P_{XZ} is the probability of a molecule of X getting to Z. P_{XZ} can be separated into the probabilities of a molecule getting from X to Y (P_{XY}), Y to Z (P_{YZ}), and Y to X (P_{YX})

$$P_{XZ} = P_{XY}P_{YZ}[1 + P_{XY}P_{YX} + (P_{XY}P_{YX})^2 + (P_{XY}P_{YX})^3 + \cdots] \quad (11)$$

Because $1 + c + c^2 + \cdots = (1 - c)^{-1}$ if $c < 1$

$$P_{XZ} = P_{XY}P_{YZ}(1 - P_{XY}P_{YX})^{-1} \quad (12)$$

P_{XY}, P_{YZ}, and P_{YX} equal $k_Y/(k_Y + k_{-X})$, $k_Z/(k_Z + k_{-Y})$, and $k_{-Y}/(k_Z + k_{-Y})$, respectively. Thus

$$k_2 = \frac{k_X\left(\frac{k_Y}{k_Y + k_{-X}}\right)\left(\frac{k_Z}{k_Z + k_{-Y}}\right)}{1 - \frac{k_Y k_{-Y}}{(k_Y + k_{-X})(k_Z + k_{-Y})}} \quad (13)$$

Upon rearrangement eq 13 becomes

$$1/k_2 = 1/k_X + 1/k_Y K_X + 1/k_Z K_X K_Y \quad (14)$$

where $K_X = k_X/k_{-X}$ and $K_Y = k_Y/k_{-Y}$. If k_X and k_Y have both a solvent (k^S) and buffer (k^B[buffer]) component and if $k_A = k_X{}^S$, $k_{AC} = k_X{}^B$, $k_D = k_Y{}^S K_X$, $k_{DC} = k_Y{}^B K_X$, and $k_B = k_Z K_X K_Y$, then eq 14 becomes eq 1 of the text, because parallel reactions are additive. The pattern of eq 14 is applicable to steady-state series reactions of any length.

(33) Massey, V.; Palmer, G. *J. Biol. Chem.* **1962**, *237*, 2347. Massey, V.; Veeger, C. *Biochim. Biophys. Acta* **1961**, *48*, 33. Staal, G. E. J.; Veeger, C. *Ibid.* **1969**, *185*, 49. Massey, V.; Williams, C. H. *J. Biol. Chem.* **1965**, *240*, 4470. Zanetti, G.; Williams, C. H.; Massey, V. *Ibid.* **1968**, *243*, 4013.

(34) Coleman, R. F.; Black, S. *J. Biol. Chem.* **1965**, *240*, 1796. Casola, L.; Brumby, P. E.; Massey, V. *Ibid.* **1966**, *241*, 4977. Massey, V.; Veeger, C. *Biochim. Biophys. Acta* **1960**, *40*, 184.

(35) Schulz, G. E.; Schirmer, R. H.; Sachsenheimer, W.; Pai, E. F. *Nature (London)* **1978**, *273*, 120.

(36) Plotkin, S., personal communication.

(37) Maeda, H.; Glaser, C. B.; Meienhofer, J. *Biochem. Biophys. Res. Commun.* **1970**, *39*, 1211.

(38) Welsh, K. M.; Creighton, D. J.; Klinman, J. P. *Biochemistry* **1980**, *19*, 2005.

(39) See discussion of the instability of disulfide anion radicals in the preceding paper.[2]